ELSEVIER

Biochimica et Biophysica Acta 1459 (2000) 467–474

BIOCHIMICA ET BIOPHYSICA ACTA

BBA

www.elsevier.com/locate/bba

# The cytochrome $b_6f$ complex: structural studies and comparison with the $bc_1$ complex

Cécile Breyton *

*Max-Planck Institute of Biophysics, Department of Structural Biology, Heinrich-Hoffmann-Strasse 7, D-60528 Frankfurt am Main, Germany*

Received 22 May 2000; accepted 12 June 2000

**Abstract**

Electron crystallography of the chloroplastic $b_6f$ complex allowed the calculation of projection maps of crystals negatively stained or embedded in glucose. This gives insights into the overall structure of the extra- and transmembrane domains of the complex. A comparison with the structure of the $bc_1$ complex, the mitochondrial homologue of the $b_6f$ complex, suggests that the transmembrane domains of the two complexes are very similar, confirming the structural homology deduced from sequence analysis. On the other hand, the extramembrane organisation of the *c*-type cytochrome and of the Rieske protein seems quite different. Nevertheless, the same type of movement of the Rieske protein is observed in the $b_6f$ as in the $bc_1$ complex upon the binding of the quinol analogue stigmatellin. Crystallographic data also suggest movements in the transmembrane domains of the $b_6f$ complex, which would be specific of the $b_6f$ complex. 

*Keywords:* Cytochrome $b_6f$ complex; Cytochrome $bc_1$ complex; Electron crystallography; Stigmatellin; Membrane protein; *Chlamydomonas reinhardtii*

## 1. Introduction

In the photosynthetic electron transfer chain, the cytochrome $b_6f$ complex plays a central role: it accepts electrons from plastoquinol, a liposoluble two-electron carrier reduced by photosystem II, and transfers them to plastocyanin, a lumenal one-electron carrier that reduces photosystem I. This transfer is associated with proton translocation across the thylakoid membrane. Thus, the $b_6f$ complex contributes to the formation of the proton gradient that is utilised by the ATP-synthase to synthesise ATP.

Three of the eight subunits of the $b_6f$ complex bear the prosthetic groups necessary for the electron transfer: cytochrome $b_6$, with its two *b*-type haems ($E_m = -84$ mV and $-158$ mV [1]), cytochrome *f* that covalently binds a *c*-type haem ($E_m = +330$ mV [1]), and the Rieske protein, bearing a [$Fe_2S_2$] cluster ($E_m = +290$ mV [2]). The Rieske protein and cytochrome *f* form the so-called high-potential path, whereas the two haems of cytochrome $b_6$, located on the opposite side of the membrane, form the low-potential path. Furthermore, subunit IV, together with the Rieske protein and cytochrome $b_6$, participate in the formation of the plastoquinol binding pocket ($Q_o$) on the lumen side of the membrane [3]. A quinone-binding site ($Q_i$) is also predicted on the other side of the membrane. The $b_6f$ complex also

* Fax: +49 (69) 96769359;
E-mail: breyton@mpibp-frankfurt.mpg.de

0005-2728/00/$ – see front matter 
PII: S0005-2728(00)00185-7

has another three or four small subunits, the products of the *petG*, *L*, *M* and *N* genes [1,4–8], and two additional prosthetic groups, a chlorophyll *a* molecule and a β-carotene [9,10].

A turnover of the $b_6f$ complex consists of the oxidation of a plastoquinol molecule at the $Q_o$ site, leading to the expulsion of two protons in the lumen and the injection of one electron into the high-potential path, where it finally reduces plastocyanin, and of the other one in the low-potential path. Following a second turnover, both *b* haems are reduced; they are then oxidised by a quinone molecule at the $Q_i$ site, resulting in the uptake of two protons in the stroma. This mechanism, the so-called 'Q-cycle', proposed by Mitchell [11] and later modified by Crofts et al. [12], has been largely confirmed by the structure of the $bc_1$ complex, the respiratory analogue of the $b_6f$ complex [13–16]. These two types of complex share not only the same function of electron transfer and proton translocation, but also a number of structural homologies: the four main prosthetic groups are the same in both types of complex, and there is strong sequence homology between cytochrome $b_6$, subunit IV and the Rieske protein of the $b_6f$ complex, and the N- and C-terminal parts of cytochrome *b*, and the Rieske protein of the $bc_1$ complex respectively. Cytochrome $c_1$ and cytochrome *f*, on the other hand, which both are *c*-type cytochromes, do not share any sequence homology although they have the same function within the complexes. Spectroscopic, EPR and redox properties of the haems and of the iron-sulfur cluster are similar (reviewed e.g. in [17]), and some inhibitors affect both complexes equally, especially the inhibitors of the $Q_o$ site, as stigmatellin or MOA-stilbene (reviewed in [18–21]).

## 2. Crystallisation and insights into the structure of the $b_6f$ complex

### 2.1. Purification and stabilisation of the $b_6f$ complex

The $b_6f$ complex from higher plants or from unicellular algae is isolated as an active dimer ([22,23] and references therein), whereas the complex from cyanobacteria purifies as a monomer [24,25]. With that exception, monomerisation appears to be the result of the destabilisation of the complex, as the monomer is inactive and has lost at least the Rieske protein and the chlorophyll molecule [22,23]. The $b_6f$ complex is quite sensitive to its manipulation in detergent solution, and delipidation has turned out to be a critical step during purification: lipids need to be added, or the complex has to be manipulated at detergent concentrations very close to their critical micellar concentration in order to prevent irreversible monomerisation [22,23].

Whether the dimeric state of the $b_6f$ complex is functionally important is not yet known, but the structure of the $bc_1$ complex suggests that the dimer is structurally fundamental. Indeed, to mention the most obvious feature, the transmembrane anchor and the extramembrane domain of the same Rieske protein belong to the two different monomers within the $bc_1$ dimer [13–15].

### 2.2. Crystallisation of the $b_6f$ complex

To date, no good three-dimensional crystals of the whole $b_6f$ complex could be grown despite ongoing efforts, so that no atomic model of the complex is available. However, the two extramembrane domains of the complex have been crystallised, and atomic models of the soluble part of cytochrome *f* of turnip and of *Phormidium laminosum* [26–28], and of the Rieske protein of spinach [29] have been obtained. The structure of cytochrome *f* is particularly interesting, as it has no homology whatsoever with its functional homologue cytochrome $c_1$ in the $bc_1$ complex. In particular, a water channel could be resolved within cytochrome *f* that is proposed to trace a path for proton release from the $Q_o$ site [30].

An alternative method to obtain structural information on proteins is the electron crystallography of two-dimensional (2D) crystals: crystals of the $b_6f$ complex from *Chlamydomonas reinhardtii* can be grown after addition of detergent solubilised lipids to the purified complex, complete removal of the detergent with Bio-Beads, and three cycles of freezing and thawing [31]. This procedure does not produce single layer 2D crystals, but rather stacks of 2D crystals, i.e. very thin type I 3D crystals. The layers (usually 3–5) are in perfect register, so that projection maps of the complex can be calculated and interpreted [31,32]. Such crystals cannot be used for a

3D reconstruction of the molecule, as the contributions from different layers overlap when the crystals are tilted in the microscope (however, see [33]). Projection maps, however, can be informative, and given the different techniques to observe the sample in the electron microscope, different parts of the crystal contribute to the signal: whereas negative stain mainly outlines the extramembrane domains of the complex, a map of unstained crystals observed at very low temperatures by electron cryo-microscopy will be dominated by the transmembrane helices of the structure.

### 2.3. Insights into the structure of the $b_6f$ complex

The $b_6f$ complex crystallises as a dimer, in a unit cell of $a=180$ Å, $b=74$ Å, and $\gamma=90°$, with $p22_12_1$ symmetry [31,32,34]. Fig. 1A shows the projection maps of a dimer of the $b_6f$ complex in negative stain, at 15 Å resolution. Within a monomer, two densities are resolved, the one furthest away from the dimer axis probably corresponding to cytochrome *f*, whereas the smaller one closer to the monomer-monomer interface would correspond to the Rieske protein (see [31,34] and below).

Fig. 1B shows the projection map of a $b_6f$ dimer calculated from crystals embedded in glucose and observed at liquid helium temperature at 10 Å resolution. Here, densities are resolved that have diameters and spacings compatible with the presence of α-helices. The two maps are very different (Fig. 1C) due to the two distinct methods used to contrast the $b_6f$ crystals. They give complementary information.

## 3. Comparison with the $bc_1$ complex

As $b_6f$ and $bc_1$ complexes share functional and sequence homology, comparisons of the two structures in projection at similar resolution (calculated from the PBD coordinates 1BCC for the $bc_1$ complex from chicken) are instructive.

### 3.1. The transmembrane domains

The cryo-projection map of the $b_6f$ complex can be compared to a calculated projection of the transmembrane region of the $bc_1$ complex viewed form the matrix or the intermembrane space (these two views are the mirror images of one another). In a first study, it was not possible to distinguish between the two orientations as the resolution of the $b_6f$ cryo-projection map was not isotropic [32]. Thus a new map, that included isotropic data to 10 Å resolution, was calculated (Fig. 1B, [34]). This map is compared to a calculated projection map of the transmembrane domain of the $bc_1$ complex at the same resolution (Fig. 1E). For the comparison, only the eight transmembrane helices of cytochrome *b* and the transmembrane anchors of the Rieske protein and of cytochrome $c_1$ were considered. An x shows the position of the other transmembrane subunits of the $bc_1$ complex that have no counterparts in the $b_6f$ complex. As shown in Fig. 1H, the comparison is very satisfactory in the orientation where the $bc_1$ projection is viewed from the matrix side of the complex, confirming the preferred orientation discussed in [32]: the complexes taken as dimers superimpose exactly, suggesting that the transmembrane organisation of the two types of *bc* complexes is very similar.

Moreover, we note the very good superimposition of an important proportion of densities (mainly in the heart of the complex): helices A to E of cytochrome *b* and of the anchor of cytochrome $c_1$ with densities of the $b_6f$ map. Whereas the superimposition for helices F and G is less satisfactory, the exact superimposition of the density of the cytochrome *b* helix H, which has no sequence homologue in the $b_6f$ complex, with a density of the $b_6f$ map is interesting. This suggests that the presence of a helix at this position is structurally important, and that in the $b_6f$ complex it would be occupied by one of the small subunits. The same conclusion can be drawn regarding one of the additional subunits of the $bc_1$ complex, which superimposes with the position of the isolated peak in the $b_6f$ map. It is to be noted though that this subunit is not present in all $bc_1$ complexes.

Also interesting to note is the superimposition of the elongated density of the tilted anchor of the $bc_1$ Rieske protein with an elongated density in the $b_6f$ map, suggesting that the $b_6f$ Rieske protein has a transmembrane anchor as in the $bc_1$ complex. This point has been controversial given biochemical anal-

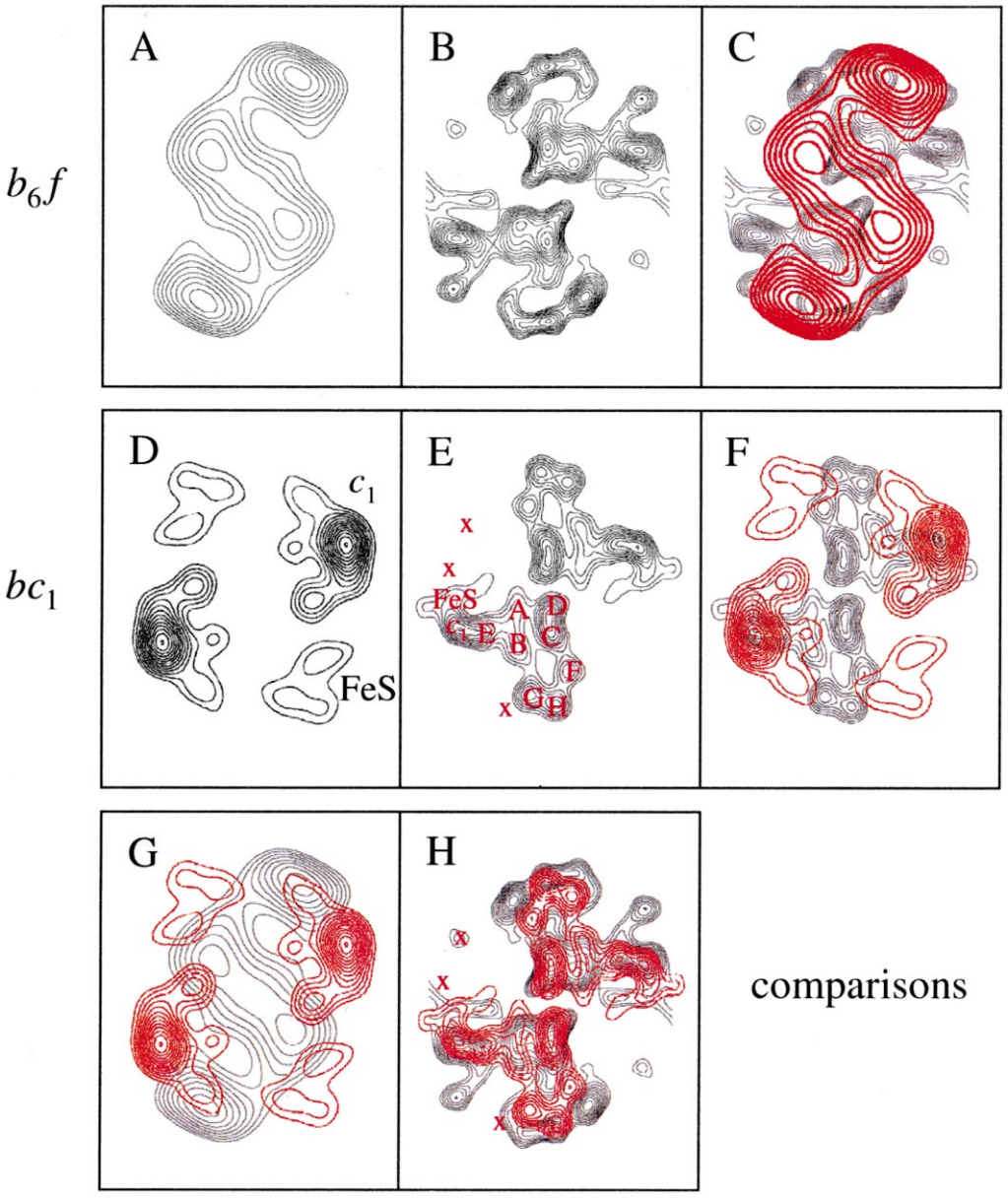


Fig. 1. Overviews and comparisons of the extra- and transmembrane domains of the $b_6f$ and $bc_1$ complexes. Projection map of the $b_6f$ complex in negative stain at 15 Å resolution (A) and embedded in glucose at 10 Å resolution (B). (C) Superimposition of the $b_6f$ negative stain and cryo maps. (D) Calculated projection map of cytochrome $c_1$ and the Rieske protein of the $bc_1$ complex at 15 Å resolution. (E) Calculated projection map of the transmembrane helices of the $bc_1$ complex at 10 Å resolution (the coordinates of the 1BCC entry of the PDB was used: cyt. *b*: 30–53; 75–103; 111–136; 172–203; 222–248; 289–308; 321–341; 347–370; cyt. $c_1$: 204–225; Rieske: 34–59; the positions of the transmembrane helices of subunits 7, 10 and 11 from bovine heart mitochondria are marked with an x). (F) Superimposition of extra- and transmembrane domains of the $bc_1$ complex. (G) Superimposition of the negative stain map of the $b_6f$ complex and the map of the extramembrane domains of the $bc_1$ complex. (H) Superimposition of cryo-map of the $b_6f$ complex and the map of the transmembrane domains of the $bc_1$ complex. In all representations, the $bc_1$ complex is seen from the matrix.

ysis: the Rieske protein from *C. reinhardtii* can be extracted from the membrane by chaotropic agents and is not aggregated when in aqueous solution in the absence of detergent (for a discussion, see [35,36] and references therein). The additional densities observed in the $b_6f$ map would correspond to contributions of the extramembrane domains and/or to the remaining small subunits.

### 3.2. The extramembrane domains

Fig. 1D shows the projection map of the extramembrane domains of cytochrome $bc_1$ complex calculated at 15 Å resolution. Cytochrome $c_1$ is projected as a large density, whereas the projection of the Rieske protein is much smaller. As a comparison to the $b_6f$ complex (Fig. 1C), the overlay of the trans- and extramembrane domains of the $bc_1$ is shown in Fig. 1F.

Fig. 1G shows the comparison of the extramembrane domain of the $bc_1$ complex with the negative stain map of the $b_6f$ complex. The orientation of the two maps is identical to that which gives the most satisfactory superimposition of the transmembrane region (see above), the $bc_1$ is seen from the matrix.

It is striking that the superimposition is far from satisfactory. The $c_1$-$c_1$ distance is smaller than the *f*-*f* distance and the $c_1$-$c_1$ axis is rotated with respect to the *f*-*f* axis, and the Rieske-Rieske distance is greater in the $bc_1$ than in the $b_6f$ complex. Whereas the positions of the Rieske proteins are rather similar, which is consistent with the similarity of the transmembrane regions and thus of the position of site $Q_o$, the positions of the *c*-type cytochrome are quite different. This can be explained by the lack of sequence and structural homology between the two proteins.

These data are consistent with the spectroscopic analysis of Schoepp et al. [37], where linear and circular dichroism results show that the *b* haems in the $b_6f$ and $bc_1$ complexes have similar arrangement, whereas the haems of cytochromes *f* and $c_1$ have different orientations.

Soriano et al. [30] have recently proposed that cytochrome *f* would lie flat on the transmembrane region, so as to mimic the arrangement of cytochrome $c_1$ and subunit 8, the hinge protein that contributes to the binding of cytochrome *c* in the $bc_1$ complex. However, this arrangement does not seem compatible with the position of the extramembrane domains of the $b_6f$ complex as seen in the negative stain map nor with the position of the *c*-type cytochrome anchoring.

## 4. Movements in the $b_6f$ complex

### 4.1. The extramembrane region

The crystal structures of the $bc_1$ complex show that the Rieske protein can assume several different positions depending upon inhibitor binding. These data suggest that this protein undergoes a substantial movement during the catalytic cycle of the complex to shuttle electrons from the quinol, located in the membrane, to the haem of cytochrome $c_1$ [13–15]. Whereas in the native structures the Rieske protein can take different positions depending on the crystal form, in the presence of the quinol analogue stigmatellin it is shifted to the proximal conformation, where one of the iron-sulfur ligands of the Rieske protein is in H-bond distance of the occupant of the $Q_o$ site. Fig. 2I shows the calculated projection map at 15 Å resolution of the extramembrane domains of the $bc_1$ complex crystallised without (Fig. $2I_A$) or with (Fig. $2I_B$) stigmatellin. Whereas the density corresponding to cytochrome $c_1$ does not change position, the density of the Rieske protein becomes more round and compact.

Fig. 2II shows the projection map in negative stain (15 Å) of crystals of the $b_6f$ complex grown in the absence (Fig. $2II_A$) or in the presence (Fig. $2II_B$) of stigmatellin [34]. The same phenomenon as that observed in the $bc_1$ complex occurs: the density further away from the dimer axis does not change position whereas the density closer to it is shifted away from the dimer axis and becomes more round and compact. If anything, the movement in the $b_6f$ complex seems to be more pronounced than in the $bc_1$ complex (Fig. $2I,II_C$). These data constitute the strongest evidence to attribute the density closer to the dimer axis to the Rieske subunit [34]. Moreover, they indicate that the mechanism of the $b_6f$ complex is very likely to involve a movement of the Rieske protein similar to that observed in the $bc_1$ complex (see also [38]). A map in negative stain of $b_6f$ crystals to which MOA-stilbene was added is very similar to that crystallised without inhibitor. If anything, the density corresponding to the Rieske protein is a bit more round, i.e. better defined (data not shown).

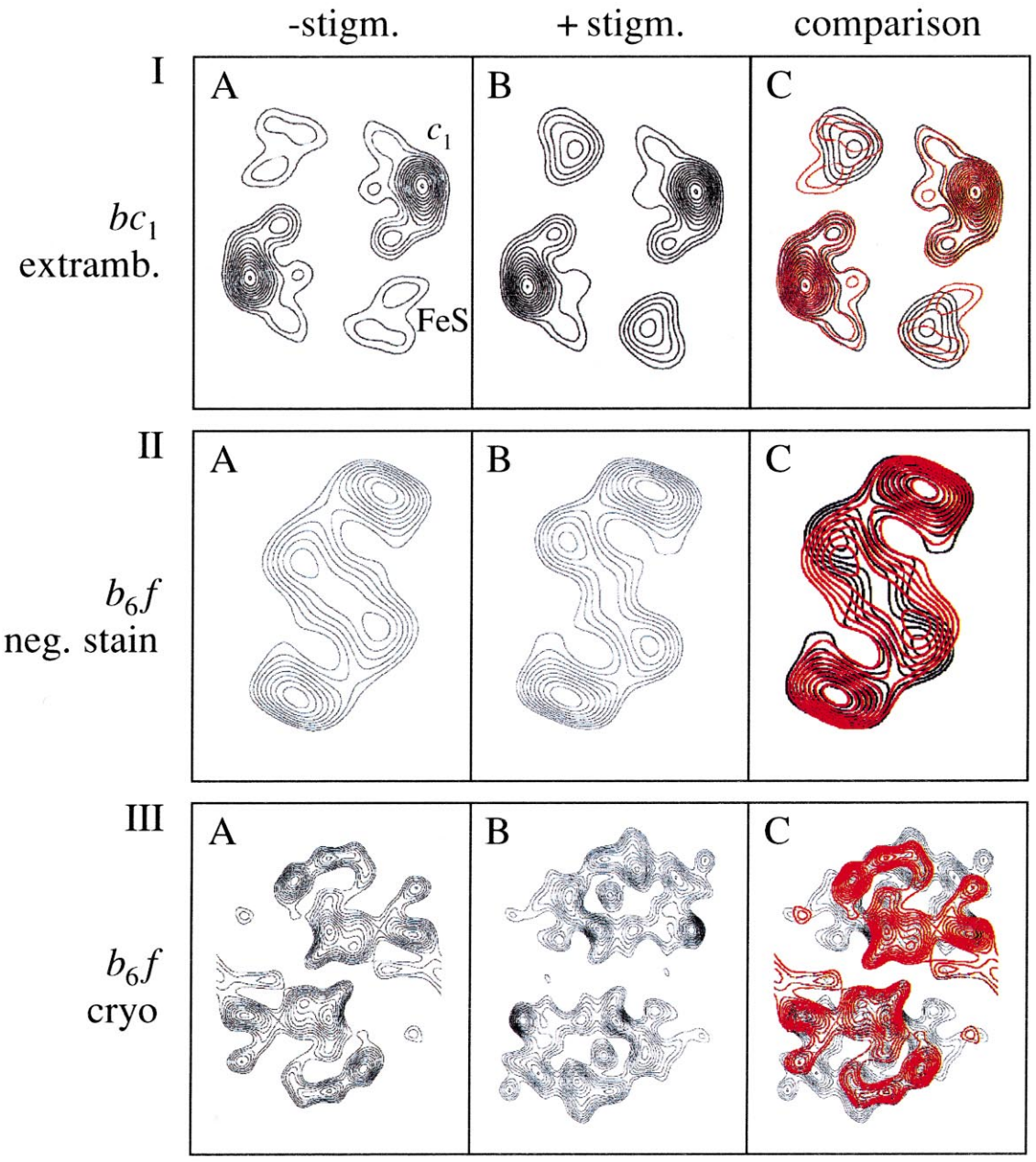


Fig. 2. Matrix of projection maps and superimpositions showing the effects of stigmatellin binding on the $bc_1$ and $b_6f$ complexes. Projections maps of $bc_1$ and $b_6f$ complexes without (A) and with stigmatellin (B). (I) Calculated projection map of the extramembrane domains of the $bc_1$ complex at 15 Å resolution. Projection maps of the $b_6f$ complex in negative stain at 15 Å resolution (II) and of crystals embedded in glucose at 10 Å resolution (III). There were no differences in the transmembrane region of the $bc_1$ complex upon binding of stigmatellin.

### 4.2. The transmembrane region

Fig. 2III shows the comparison of the projection map at 10 Å resolution in cryo of $b_6f$ crystals grown in the absence (Fig. $2III_A$) or in the presence (Fig. $2III_B$) of stigmatellin [34]. The two maps look quite different, which is unexpected, as there are absolutely no changes in the transmembrane region of the $bc_1$ complex upon binding of stigmatellin. Here, the heart of the complex remains roughly unchanged, whereas differences appear further away from the dimer axis. They suggest movements in the trans-

membrane domains of the $b_6f$ complex upon binding of the inhibitor, which may reflect the functional differences that distinguish the photosynthetic and respiratory complexes. Briefly, one can mention a difference in the mechanism, where direct proton pumping would occur in the $b_6f$ [39,40], or the role of the $b_6f$ complex in the regulation of photosynthesis ([41]; see discussion in [34]). One of the differences, however, can be explained by the ordering of the Rieske protein following stigmatellin binding. These results should be regarded as preliminary, and will have to be confirmed by the calculation of a 3D map of the $b_6f$ complex.

## 5. Conclusions and perspectives

Given the difficulty of obtaining 3D crystals of the $b_6f$ complex, the only crystallographic information available concerning the entire complex is at present provided by electron crystallography. This technique is particularly suitable to calculate maps at intermediate resolution, and the work reviewed here shows that it yields unique and useful information: comparing the $b_6f$ projection maps with calculated projection maps of the $bc_1$ complex, it is concluded that the transmembrane domains of both complexes are similar. This is in agreement with the functional and sequence homology between the subunits that are buried in the membrane and form the quinol-binding sites (see also [30]). On the other hand, the organisation of the extramembrane domains are different, although it is shown that a similar movement of the Rieske protein occurs in the $b_6f$ as in the $bc_1$ complex. This, together with the different structure of the two *c*-type cytochromes and the results obtained by Schoepp et al. [37] concerning the different organisation of the *c*-type haems, suggests that the same function (electron transfer between a quinol molecule and a soluble electron acceptor) can be achieved by different spatial organisations of the redox centres. This represents therefore a major point of interest in the study of the structure-function relationship of the $b_6f$ complex. To confirm the negative stain results, ruling out possible artefacts due to differential accumulation of the stain in the crystals, atomic force microscopy measurements will be performed. This technique gives a surface representation of the molecule (for a review, see [42]): it will not only give an independent view of the position of the two extramembrane domains, but also the handedness of the protein, i.e. the side from which the projection is seen.

Ultimately, the 3D structure of the $b_6f$ complex will have to be determined. To this end, conditions allowing the growth of true 2D crystals are being investigated using the conventional methods of slowly removing the detergent by dialysis [45]. A His-tagged $b_6f$ is available that will allow the investigation of crystal growth under a functionalised lipid monolayer at the air-water interface. New molecules such as fluorinated detergents (see i.e. [43]) or fluorinated functionalised lipids [44] will be utilised, as the presence of classical detergent will most probably solubilise the lipid interfacial monolayer.

## Acknowledgements

I warmly thank Werner Kühlbrandt and Jean-Luc Popot for their encouragement and support, Giovanni Finazzi for useful discussions, and Peter Rich for a kind gift of MOA-stilbene. Acknowledge EMBO for financial support.

## References

[1] Y. Pierre, C. Breyton, D. Kramer, J.-L. Popot, J. Biol. Chem. 270 (1995) 29342–29349.
[2] W. Nitschke, P. Joliot, U. Liebl, A.W. Rutherford, G. Hauska, A. Müller, A. Riedel, Biochim. Biophys. Acta 1102 (1992) 266–268.
[3] M.P. Doyle, L.B. Li, L. Yu, C.A. Yu, J. Biol. Chem. 264 (1989) 1387–1392.
[4] J. Haley, L. Bogorad, Proc. Natl. Acad. Sci. USA 86 (1989) 1534–1538.
[5] Y. Pierre, J.-L. Popot, C. R. Acad. Sci. Ser. III 316 (1993) 1404–1409.
[6] C. de Vitry, C. Breyton, Y. Pierre, J.-L. Popot, J. Biol. Chem. 271 (1996) 10667–10671.
[7] Y. Takahashi, M. Rahire, C. Breyton, J.-L. Popot, P. Joliot, J.-D. Rochaix, EMBO J. 15 (1996) 3498–3506.
[8] M. Hager, K. Biehler, J. Illerhaus, S. Ruf, R. Bock, EMBO J. 18 (1999) 5834–5842.
[9] Y. Pierre, C. Breyton, Y. Lemoine, B. Robert, C. Vernotte, J.-L. Popot, J. Biol. Chem. 272 (1997) 21901–21908.
[10] H. Zhang, D. Huang, W.A. Cramer, J. Biol. Chem. 274 (1999) 1581–1587.

[11] P. Mitchell, FEBS Lett. 57 (1975) 137–139.
[12] A.R. Crofts, S.W. Meinhardt, K.R. Jones, M. Snozzi, Biochim. Biophys. Acta 723 (1983) 202–218.
[13] H. Kim, D. Xia, C.A. Yu, J.Z. Xia, A.M. Kachurin, L. Zhang, L. Yu, J. Deisenhofer, Proc. Natl. Acad. Sci. USA 95 (1998) 8026–8033.
[14] S. Iwata, J.W. Lee, K. Okada, J.K. Lee, M. Iwata, B. Rasmussen, T.A. Link, S. Ramaswamy, B.K. Jap, Science 281 (1998) 64–71.
[15] Z. Zhang, L. Huang, V.M. Shulmeister, Y.I. Chi, K.K. Kim, L.W. Hung, A.R. Crofts, E.A. Berry, S.H. Kim, Nature 392 (1998) 677–684.
[16] D. Xia, C.A. Yu, H. Kim, J.Z. Xia, A.M. Kachurin, L. Zhang, L. Yu, J. Deisenhofer, Science 277 (1997) 60–66.
[17] G. Hauska, M. Schütz, M. Büttner, in: D.R. Ort, C.F. Yocum (Eds.), Oxygenic Photosynthesis: the Light Reactions, Kluwer Academic Publishers, Dordrecht, 1996, pp. 377–398.
[18] G. Hauska, W. Nitschke, R.G. Herrmann, J. Bioenerg. Biomembr. 20 (1988) 211–228.
[19] R. Malkin, Photosynth. Res. 33 (1992) 121–136.
[20] P.N. Furbacher, G.-S. Tae, W.A. Cramer, in: H. Baltcheffsky (Ed.), Origin and Evolution of Biological Energy Conservation, VCH, New York, 1996.
[21] W.A. Cramer, M.T. Black, W.R. Widger, M.E. Girvin, in: J. Barber (Ed.), The Light Reactions, Elsevier, Amsterdam, 1987, pp. 447–493.
[22] D. Huang, R.M. Everly, R.H. Cheng, J.B. Hetmann, H. Schägger, V. Sled, T. Ohnishi, T.S. Baker, W.A. Cramer, Biochemistry 33 (1994) 4401–4409.
[23] C. Breyton, C. Tribet, J. Olive, J.P. Dubacq, J.L. Popot, J. Biol. Chem. 272 (1997) 21892–21900.
[24] D. Bald, J. Kruip, E.J. Boekema, M. Rögner, in: N. Murata (Ed.), Research in Photosynthesis. Proceedings of the IXth International Congress on Photosynthesis, vol. I, Kluwer Academic Publishers, Nagoya, 1992, pp. 629–632.
[25] E.J. Boekema, A.F. Boonstra, J.P. Dekker, M. Rögner, J. Bioenerg. Biomembr. 26 (1994) 17–29.
[26] S.E. Martinez, D. Huang, A. Szczepaniak, W.A. Cramer, J.L. Smith, Structure 2 (1994) 95–105.
[27] S.E. Martinez, D. Huang, M. Ponomarev, W.A. Cramer, J.L. Smith, Protein Sci. 5 (1996) 1081–1092.
[28] C.J. Carrell, B.G. Schlarb, D.S. Bendall, C.J. Howe, W.A. Cramer, J.L. Smith, Biochemistry 38 (1999) 9590–9599.
[29] C.J. Carrell, H. Zhang, W.A. Cramer, J.L. Smith, Structure 5 (1997) 1613–1625.
[30] G.M. Soriano, M.V. Pomarev, C.J. Carrell, D. Xia, J.L. Smith, W.A. Cramer, J. Bioenerg. Biomembr. 31 (1999) 201–213.
[31] G. Mosser, C. Breyton, A. Olofsson, J.L. Popot, J.L. Rigaud, J. Biol. Chem. 272 (1997) 20263–20268.
[32] P. Bron, J.J. Lacapère, C. Breyton, G. Mosser, J. Mol. Biol. 287 (1999) 117–126.
[33] D. Shi, M.R. Lewis, H.S. Young, D.L. Stokes, J. Mol. Biol. 284 (1998) 1547–1564.
[34] C. Breyton, J. Biol. Chem. 275 (2000) 13195–13201.
[35] I. Karnauchov, R.G. Herrmann, R.B. Klosgen, FEBS Lett. 408 (1997) 206–210.
[36] C. Breyton, C. de Vitry, J.-L. Popot, J. Biol. Chem. 269 (1994) 7597–7602.
[37] B. Schoepp, E. Chabaud, C. Breyton, A. Verméglio, J.-L. Popot, J. Biol. Chem. 275 (2000) 5275–5783.
[38] B. Schoepp, M. Brugna, A. Riedel, W. Nitschke, D.M. Kramer, FEBS Lett. 450 (1999) 245–250.
[39] P. Joliot, A. Joliot, Biochemistry 37 (1998) 10404–10410.
[40] F. Zito, G. Finazzi, P. Joliot, F.A. Wollman, Biochemistry 37 (1998) 10395–10403.
[41] F. Zito, G. Finazzi, R. Delosme, W. Nitschke, D. Picot, F.-A. Wollman, EMBO J. 18 (1999) 2961–2969.
[42] A. Engel, Lyubchenko, D.J. Müller, Trends Cell Biol. 9 (1999) 77–80.
[43] E. Chabaud, P. Barthelemy, N. Mora, J.L. Popot, B. Pucci, Biochimie 80 (1998) 515–530.
[44] F. Lach, C. Vénien-Bryan, A. Renault, J. Dietrich, W. Kühlbrandt, T. Jahn, M.G. Palmgren, C. Mioskowski, L. Lebeau, (2000) submitted.
[45] W. Kühlbrandt, Quart. Rev. Biophys. 25 (1992) 1–49.